EPR detection of the unstable *tert*-butylperoxyl radical adduct of the spin trap 5,5-dimethyl-1-pyrroline *N*-oxide: a combined spin-trapping and continuous-flow investigation

Clare M. Jones and Mark J. Burkitt *

Gray Cancer Institute, PO Box 100, Mount Vernon Hospital, Northwood, Middlesex, UK HA6 2JR. E-mail: burkitt@gci.ac.uk; Fax: +44 (0)1923-835210; Tel: +44 (0)1923-828611

Received (in Cambridge, UK) 6th August 2002, Accepted 27th September 2002
First published as an Advance Article on the web 28th October 2002

The EPR spin-trapping technique has been applied extensively to the detection of organic peroxyl radicals in biological systems. The most widely used spin trap is 5,5-dimethyl-1-pyrroline *N*-oxide (DMPO), of which adducts displaying EPR signals with a(N) ~1.43 mT, a(β-H) ~1.17 mT and a(γ-H) ~0.12 mT have been routinely assigned to trapped peroxyl radicals. Recently, however, it has been shown that such signals are from alkoxyl radical adducts, generated during the decomposition of peroxyl radical adducts. In the present investigation, we have used the Ce^{IV}–*tert*-butyl hydroperoxide redox couple as an efficient means of generating peroxyl radicals ($^tBuOO^\bullet$) in a fast-flow, dielectric mixing-resonator. This allowed the direct, EPR observation of $^tBuOO^\bullet$ radicals, as well as a short-lived radical adduct upon the inclusion of DMPO. Although the hyperfine coupling constants for this adduct were essentially indistinguishable from those of the more stable methoxyl radical adduct (DMPO–$^\bullet$OMe), it is reasoned on kinetic and chemical grounds why this species is believed to be the *tert*-butylperoxyl radical adduct (DMPO–$^\bullet OO^tBu$). The rate constant for $^tBuOO^\bullet$ spin trapping was estimated to be *ca.* 30 M^{-1} s^{-1}, which is considerably lower than the value of > 10^3 M^{-1} s^{-1} proposed recently by Honeywill and Mile (*J. Chem. Soc., Perkin Trans. 2*, 2002, 569), who concluded that alkylperoxyl radicals form only diamagnetic adducts, *via* their multiple addition to DMPO. Complementary spin-trapping experiments in a static system resulted in detection of the methoxyl and *tert*-butoxyl radical adducts of DMPO (generated *via* DMPO–$^\bullet OO^tBu$ decomposition), as well as the three-electron oxidation product 5,5-dimethyl-1-pyrrolidone-2-oxyl. These findings demonstrate that the chemistry underlying the generation of the radical adducts detected by spin trapping in peroxyl-radical generating systems must be interpreted with extreme caution. Furthermore, through the direct observation of the DMPO–$^\bullet OO^tBu$ adduct under continuous-flow conditions, this work gives support to earlier suggestions that DMPO peroxyl radical adducts are formed, but are too unstable to be detected under the conditions employed in typical spin-trapping studies.

Introduction

Peroxyl radicals are important intermediates in autoxidation reactions of both chemical and biological importance.[1–3] In addition to their role in the polymerisation of paints ('drying'), the species serve as radical-transfer agents during the propagation of lipid peroxidation in foodstuffs and biological membranes. This latter process has been associated with various disease processes,[4] including the oxidation of lipoprotein particles during atherosclerosis.[5] Peroxyl radicals may be formed *via* the direct addition of molecular oxygen to carbon-centred radicals (*e.g.*, during the 'fixation' of radiation damage[6] and during fatty acid oxidation by lipoxygenases[7]). Alternatively, the species can be generated *via* the one-electron oxidation of organic hydroperoxides, of which *tert*-butyl hydroperoxide (^tBuOOH) is perhaps the most widely studied model compound, eqn. (1):

$$(CH_3)_3COOH \longrightarrow (CH_3)_3COO^\bullet + H^+ + e^- \qquad (1)$$

Both secondary and tertiary alkylperoxyl radicals have been observed directly by EPR spectroscopy in conjunction with either *in situ* photolysis or continuous-flow systems.[7–10] The *tert*-butylperoxyl radical has also been observed directly during the interaction of haematin with ^tBuOOH.[11] However, due to the instability of peroxyl radicals, particularly secondary alkylperoxyl radicals, the most widely used approach to their observation in biological systems is spin trapping with the nitrone 5,5-dimethyl-1-pyrroline *N*-oxide (DMPO) (Fig. 1), as shown in eqn. (2) for the *tert*-butylperoxyl radical.

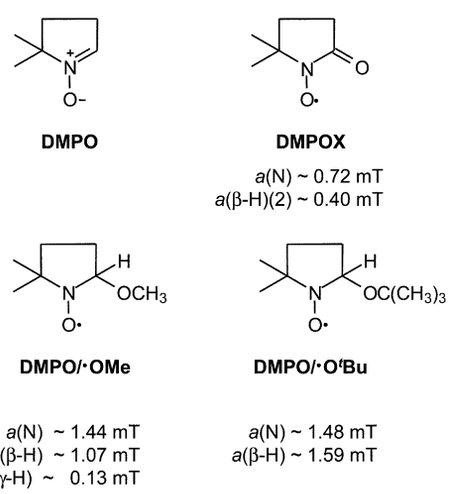

Fig. 1 Structures of DMPO and nitroxides referred to in the text. The hyperfine coupling constants of the nitroxides are typical literature values,[13,19,23,34] rather than being the precise values obtained in the present study (which are given in the text).

$$(CH_3)_3COO^\bullet + DMPO \longrightarrow DMPO\text{–}^\bullet OOC(CH_3)_3 \qquad (2)$$

 DOI: 10.1039/b207709b

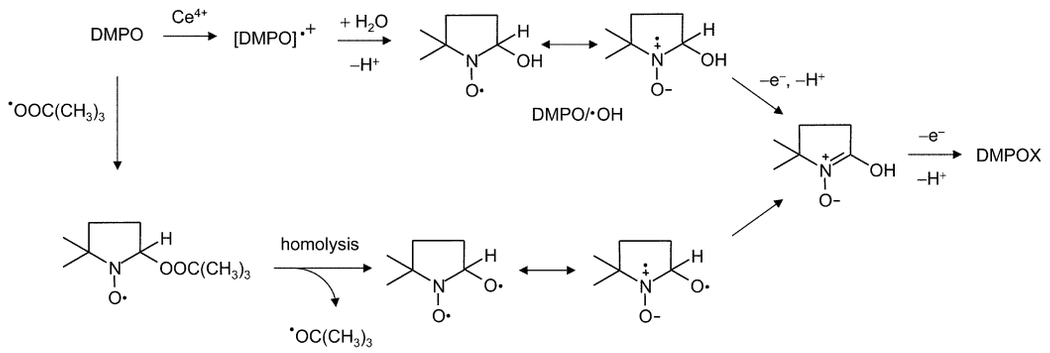

Scheme 1 Suggested reaction scheme for the oxidation of the spin trap DMPO to the nitroxide DMPOX by Ce^{IV} and the *tert*-butylperoxyl radical. It is proposed that each of the one-electron oxidation steps is brought about by the metal ion. The structures of DMPO and DMPOX are given in Fig. 1.

For over 20 years, numerous EPR spectra have been attributed to peroxyl radical adducts of DMPO based only on their similarity to the spectrum of the superoxide adduct [DMPO–$^{\bullet}$OOH, for which a(N) ~1.43 mT, a(β-H) ~1.17 mT and a(γ-H) ~0.12 mT[12]] and insensitivity to superoxide dismutase.[11,13–18] Recently, however, the assignment of such spectra to peroxyl radical adducts has been brought into serious question. Prompted by the fact that the hyperfine coupling constants (hfcc) of the methoxyl radical adduct of DMPO (DMPO–$^{\bullet}$OMe), which is readily synthesised, are the same as those reported for the *tert*-butylperoxyl adduct (DMPO–$^{\bullet}$OO^{t}Bu), Dikalov and Mason have provided strong evidence that in all previous studies the spectra assigned to DMPO peroxyl radical adducts are in fact from alkoxyl radical adducts.[19,20] The authors suggested that the peroxyl radical adducts of all spin traps are too unstable to be detected at room temperature, as demonstrated earlier for the trap *N*-*tert*-butyl-α-phenylnitrone.[21,22] The DMPO–$^{\bullet}$OO^{t}Bu adduct is proposed to undergo rapid degradation with the liberation of free *tert*-butoxyl radicals, which are either trapped by excess DMPO or undergo β-scission to the methyl radical as shown in reaction (3). The mechanistic aspects of DMPO–$^{\bullet}$OO^{t}Bu decomposition were not discussed in great detail by Diklov and Mason, but will be addressed below (Results and discussion section and Scheme 1). The methoxyl radical adduct, the species previously mistaken for DMPO–$^{\bullet}$OO^{t}Bu, is generated *via* oxygen addition to the methyl radical as in reactions (4)–(9):[19]

$$(CH_3)_3CO^{\bullet} \longrightarrow (CH_3)_2CO + {}^{\bullet}CH_3 \quad (3)$$

$$^{\bullet}CH_3 + O_2 \longrightarrow {}^{\bullet}OOCH_3 \quad (4)$$

$$^{\bullet}OOCH_3 + DMPO \longrightarrow [DMPO\text{–}{}^{\bullet}OOCH_3] \longrightarrow \longrightarrow DMPO\text{–}{}^{\bullet}OCH_3 \quad (5)$$

$$2\ {}^{\bullet}OOCH_3 \longrightarrow CH_3OOOOCH_3 \quad (6)$$

$$CH_3OOOOCH_3 \longrightarrow CH_2O + CH_3OH + O_2 \quad (7)$$

$$CH_3OOOOCH_3 \longrightarrow 2\ {}^{\bullet}OCH_3 + O_2 \quad (8)$$

$$DMPO + {}^{\bullet}OCH_3 \longrightarrow DMPO\text{–}{}^{\bullet}OCH_3 \quad (9)$$

In addition to their release from DMPO peroxyl radical adducts, alkoxyl radicals are generated *via* the one-electron reduction of organic hydroperoxides, *e.g.*, eqn. (10) for generation from ^{t}BuOOH:

$$(CH_3)_3COOH + e^- \longrightarrow (CH_3)_3CO^{\bullet} + OH^- \quad (10)$$

The EPR spectrum of the DMPO–$^{\bullet}$O^{t}Bu radical adduct [a(N) ~1.48 mT, a(β-H) ~1.59 mT] is readily distinguished from that of DMPO–$^{\bullet}$OMe.[23] Depending on the concentration of the spin trap, detection of the DMPO–$^{\bullet}$O^{t}Bu adduct is often accompanied by the observation of signals from DMPO–$^{\bullet}$Me (and DMPO–$^{\bullet}$OMe) resulting from reactions (3)–(9).[23] It is clear, therefore, that considerable caution must be exercised in the analysis of EPR spectra containing multiple signals from organic hydroperoxide-derived radical adducts of DMPO.

Although strong evidence exists for the decomposition of DMPO peroxyl radical adducts to alkoxyl radical adducts,[19,20] this process has not been observed directly: there would appear to be no reported EPR spectrum of an authentic DMPO alkylperoxyl radical adduct. In the present investigation, we have attempted to obtain and characterise the EPR spectrum of the DMPO–$^{\bullet}$OO^{t}Bu adduct. The approach taken has been to generate peroxyl radicals *via* the continuous, rapid mixing of ^{t}BuOOH and Ce^{IV} in a small-scale EPR flow cavity. Using this well-defined system, the ^{t}BuOO$^{\bullet}$ radical can be observed directly. The introduction of DMPO into the flow system permitted the detection of a short-lived radical adduct, the decay of which was monitored by decreasing the flow rate.

Experimental

Reagents

Sulfuric acid was purchased as a 1 M solution from Fisher Scientific UK (Loughborough, Leics). All other chemicals were from Sigma-Aldrich UK (Poole, Dorset). The Ce^{IV} salt used was cerium ammonium nitrate. *tert*-Butyl hydroperoxide was purchased as a 70% aqueous solution. DMPO was purified by vacuum distillation (Kugelrohr) and stored at −80 °C.

Stoichiometry of ^{t}BuOOH oxidation by Ce^{IV}

Aliquots from a 20 μM solution of $(NH_4)_2Ce(NO_3)_6$, prepared in 0.4 M sulfuric acid, were added to an aqueous solution of ^{t}BuOOH, at an initial peroxide concentration of 2.5 μM. After thorough mixing, aliquots were removed and the concentration of remaining ^{t}BuOOH determined using the FOX1 assay (version including sorbitol).[24] Due to reported differences in the behaviour of H_2O_2 and organic hydroperoxides in this assay,[25] our standard curve was prepared using standard solutions of ^{t}BuOOH, being linear over the range of peroxide concentrations used (0–5 μM).

Stopped-flow electronic absorption spectroscopy

The rate of reaction between Ce^{IV} and ^{t}BuOOH was measured by monitoring the decrease in absorption at 380 nm by Ce^{IV} using a stopped-flow apparatus (model SF-61 DX2, Hi-Tech Scientific, Salisbury, Wilts). Light absorption at this wavelength by Ce^{III} and ^{t}BuOOH is negligible. Reagents were prepared in 0.4 M sulfuric acid and reactions carried out at 25 ± 1 °C. The initial, post-mixing concentration of $(NH_4)_2Ce(NO_3)_6$ was 0.5 mM. ^{t}BuOOH was present in excess, at the final concentrations shown in Fig. 4. Pseudo first-order rate constants were

determined from fits performed using software provided with the instrument.

EPR spectroscopy

The *tert*-butylperoxyl radical was generated by the continuous mixing of solutions of Ce^{IV} and ^{t}BuOOH in a dielectric mixing-resonator (model ER 4117 D-MVT, Bruker UK Ltd, Coventry) housed in a Bruker EMX spectrometer, operating at the following instrument settings: modulation frequency, 100 kHz; sweep width, 12 mT; microwave power, 20 mW; modulation amplitude, 0.5 mT; sweep time, 84 s; time constant, 41 ms and receiver gain, 2×10^4. The $(NH_4)_2Ce(NO_3)_6$ and ^{t}BuOOH stock solutions were each prepared in 0.4 M sulfuric acid to give final (post-mixing) concentrations of 0.5 mM and 0.23 M, respectively. Flow through the cavity was maintained using a two-stream syringe infusion pump (model 22, Harvard Apparatus Ltd, Edenbridge, Kent). The combined flow-rate was varied over the range shown in the appropriate figure legends. All kinetic experiments were performed at 25 ± 1 °C.

For continuous-flow experiments involving the use of DMPO, the spin trap was added to the ^{t}BuOOH solution, which was prepared in 0.2 M sodium phosphate buffer (pH 7) and flowed against $(NH_4)_2Ce(NO_3)_6$ at the concentrations given below. The final, post-mixing pH of the reaction was 2.3. In such experiments, the following modifications were made to the instrument settings: sweep width, 7 mT; modulation amplitude, 0.2 mT; sweep time, 42 s; time constant, 82 ms and receiver gain, 4×10^4. Additional spin-trapping experiments were carried out using a conventional, cylindrical cavity (HS model, Bruker UK Ltd) and a quartz flat-cell. These reactions contained 5 mM $(NH_4)_2Ce(NO_3)_6$, 0.25 M ^{t}BuOOH and 0.8 M DMPO in 0.4 M sulfuric acid. The following changes were made to the instrument settings given above: sweep width, 8 mT; modulation amplitude, 0.1 mT; sweep time, 84 s; time constant, 20 ms and receiver gain, 4×10^4 (four spectra were accumulated and added).

The spectrometer field calibration was checked using the signal from a dilute solution of Fremy's salt [(a(N) = 1.3091 mT [26]] and was accurate to within ± 0.005 mT for both resonators. Hyperfine coupling constants were determined from spectral simulations performed using software available through the Internet (http://epr.niehs.nih.gov/) and described elsewhere.[27]

Results and discussion

Stoichiometry of ^{t}BuOOH oxidation by Ce^{IV}

The one-electron oxidation of ^{t}BuOOH by Ce^{IV} in continuous-flow EPR systems has been used as an efficient method for the generation of the ^{t}BuO$^{\bullet}$ radical as given in reaction (11).[10,28,29]

$$Ce^{4+} + (CH_3)_3COOH \longrightarrow (CH_3)_3COO^{\bullet} + Ce^{3+} + H^{+} \quad (11)$$

The hydrated ceric ion $[Ce(OH_2)_n]^{4+}$ is a fairly strong acid and, except at very low pH, undergoes hydrolysis and polymerisation. Therefore, in the studies reported here, the Ce^{IV} salt was dissolved in 0.4 M H_2SO_4, in which the metal ion will be present as $[Ce(SO_4)_3]^{2-}$. Given the high $E°$ of the $[Ce(SO_4)_3]^{2-}/[Ce(SO_4)_3]^{3-}$ couple (1.44 V),[30] it is considered unlikely that the Ce^{III} generated in reaction (11) can participate in further redox reactions. However, in order establish experimentally whether or not Ce^{III} can be oxidised by ^{t}BuOOH and thereby undergo redox cycling (which would need to be considered in any kinetic analysis of ^{t}BuO$^{\bullet}$ formation), titrations were performed to determine the stoichiometry of ^{t}BuOOH oxidation by $[Ce(SO_4)_3]^{2-}$. Aliquots of Ce^{IV} were added to a solution of ^{t}BuOOH and the concentration of peroxide remaining determined by its ability to oxidise an acidic solution of Fe^{II} to Fe^{III}, resulting in formation of the Fe^{III}–xylenol orange complex ($\varepsilon_{560\ nm} = 1.5 \times 10^4\ M^{-1}\ cm^{-1}$).[24] Titration of ^{t}BuOOH with $[Ce(SO_4)_3]^{2-}$ showed that 2 equivalents of Ce^{IV} are required to remove each equivalent of the peroxide (Fig. 2), suggesting that Ce^{III} is not oxidised by ^{t}BuOOH.

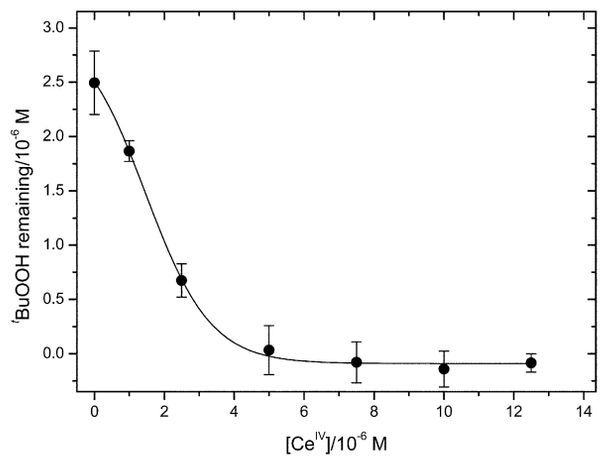

Fig. 2 Titration of the reaction between Ce^{IV} and ^{t}BuOOH. At the final concentrations indicated, Ce^{IV} was mixed with an aqueous solution of ^{t}BuOOH, of initial concentration 2.5 μM. Aliquots were then removed and the concentration of remaining ^{t}BuOOH determined using a colorimetric assay (described in the Experimental section).

Although Ce^{IV} is itself expected to be capable of oxidising Fe^{II}, this is believed to not contribute significantly to the formation of the Fe^{III}–xylenol orange complex for three reasons. Firstly, when [Ce^{IV}] is low relative to [^{t}BuOOH], all of the Ce^{IV} will be reduced to Ce^{III} by the peroxide before the Fe^{II} is added. Secondly, when the reduction of Ce^{IV} to Ce^{III} by the peroxide is incomplete (*i.e.*, when [Ce^{IV}] > 5 μM, see Fig. 2), the concentration of Ce^{IV} remaining will be very small (*e.g.*, 5 μM when starting with 10 μM) compared with the concentration of Fe^{II} used to assay the peroxide (2.5 mM). Finally, the reaction of Ce^{IV} with excess Fe^{II} will not initiate the series of 'amplification' reactions (involving the generation of alkyl hydroperoxides from sorbitol) used to enhance the sensitivity of the assay.[24] It is concluded, therefore, that one equivalent of Ce^{IV} is reduced in the oxidation of ^{t}BuOOH to ^{t}BuOO$^{\bullet}$, which is presumably then oxidised by a second Ce^{IV} equivalent, resulting in the observed 2:1 ([Ce^{IV}]:[^{t}BuOOH]) reaction stoichiometry. Under the conditions of [^{t}BuOOH] ⩾ [Ce^{IV}] employed in the EPR experiments to be described below, it may be assumed that all of the Ce^{IV} reacts with the peroxide and that decay of the peroxyl radical is by self-reaction [reactions (12, 12a and 12b)].[29]

$$2(CH_3)_3COO^{\bullet} \longrightarrow \text{products} \quad (12)$$

$$2(CH_3)_3COO^{\bullet} \longrightarrow (CH_3)_3COOC(CH_3)_3 + O_2 \quad (12a)$$

$$2(CH_3)_3COO^{\bullet} \longrightarrow 2\,(CH_3)_3CO^{\bullet} + O_2 \quad (12b)$$

The above findings are consistent with the conclusions of Bennett who, using computer simulation, obtained good fits for the decay of ^{t}BuOO$^{\bullet}$ based on bimolecular self-reaction [reaction (12)]. Fits were not quite so good when Ce^{IV} was in excess, which was suggested may indicate reaction between ^{t}BuOO$^{\bullet}$ and the metal ion.[29]

Kinetics of *tert*-butylperoxyl radical generation and decay

In conventional EPR flow-systems, large quantities of reagents are consumed, which would preclude the inclusion of DMPO. Therefore in the present study a two-stream, dielectric mixing-resonator having an active sample volume of only 1 μl was used. An EPR signal from the ^{t}BuOO$^{\bullet}$ radical (g ~ 2.015) was

observed as solutions of Ce^{IV} and ^{t}BuOOH were pumped continuously through the resonator using a syringe-drive unit. The intensity of the signal increased with increasing flow rate (Fig. 3). In a conventional flow-system, consisting of a two- or

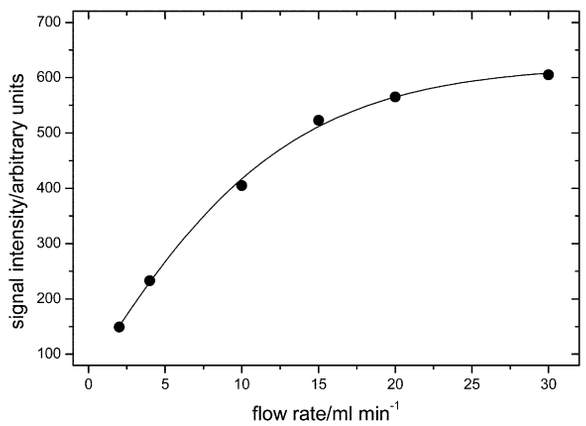

Fig. 3 Effect of flow rate on the intensity of the EPR signal from ^{t}BuOO$^{\bullet}$, observed during the continuous mixing of Ce^{IV} and ^{t}BuOOH at final concentrations of 0.5 mM and 0.23 M, respectively. The flow rates shown are the combined rates from the two reagent streams. Values are means from triplicate runs, with standard deviations less than the size of the symbols.

three-stream mixer located immediately before a quartz flat-cell, the time taken for the reagents, after mixing, to flow to the point of observation within the resonator (*i.e.*, the reaction time, t) can be determined by optical means: the flat cell and mixing chamber are placed in a spectrophotometer and the formation of $FeNCS^{2+}$ from $Fe(ClO_4)_3$ and KSCN is monitored at 460 nm. Using the known value for $k(Fe^{III} + SCN^{-})$, the value of t for a given flow rate can be determined.[31] Because the dielectric mixing-resonator consists of an integral mixing chamber and quartz capilliary tube, with no optical window, it is not possible to measure t by such means. Therefore the approach employed here was to determine t directly by EPR spectroscopy: with a knowledge of k_{11}, the rate constant for the one-electron oxidation of ^{t}BuOOH by Ce^{IV}, reaction (11), and the rate constant for the bimolecular decay of the resultant ^{t}BuOO$^{\bullet}$ radical, reaction (12), for which $2k_{12}$ is 2×10^4 M^{-1} s^{-1},[29] it is possible to determine t from the variation in EPR signal intensity with flow rate. To determine k_{11}, the reduction of Ce^{IV} by excess ^{t}BuOOH was monitored at 380 nm using stopped-flow electronic absorption spectroscopy. From the pseudo first-order plot, the second-order rate constant for reaction (11) was determined to be 1.3×10^4 M^{-1} s^{-1} (see Fig. 4,

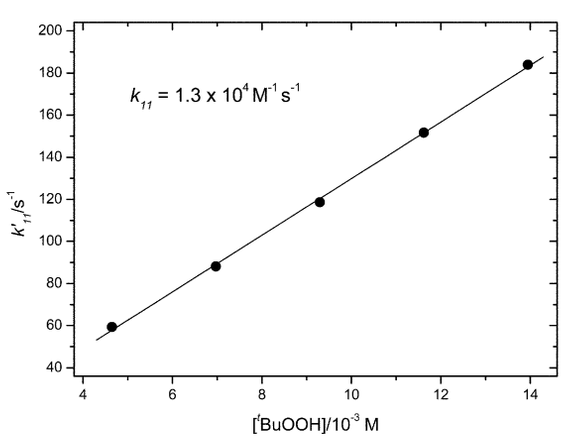

Fig. 4 Determination of the second-order rate constant (k_{11}) for the reaction between Ce^{IV} and ^{t}BuOOH using stopped-flow electronic absorption spectroscopy under pseudo first-order conditions (k'_{11} is the corresponding pseudo first-order rate constant). See text for details.

where k'_{11} is the pseudo first-order rate constant for the oxidation of ^{t}BuOOH by Ce^{IV}), which is in very good agreement with a previous determination.[29]

Czapski has proposed mathematical models for the generation and decay of radicals in EPR continuous-flow systems.[32] In one extreme case, when the rate of the initial, radical generating reaction is low, it is assumed that a steady state concentration of radicals exists at the point of observation in the cell at which the spectrum is recorded, *i.e.* radical generation is still underway when the mixed reagents have reached the observation point. In the other extreme case, it is assumed that the initial reaction is very fast and completed immediately after the reagents are mixed. In this case, the concentration of radicals detected is determined only by the rate of their decay and would be described, in the system studied here, by the eqn. (13),

$$1/[\,^{t}\mathrm{BuOO}^{\bullet}]_t = 2k_{12}t + 1/[\,^{t}\mathrm{BuOO}^{\bullet}]_o \qquad (13)$$

in which $[^{t}\mathrm{BuOO}^{\bullet}]_t$ is the concentration of peroxyl radicals at time t (*i.e.*, at the point of EPR observation) and $[\,^{t}\mathrm{BuOO}^{\bullet}]_o$ is the initial peroxyl radical concentration (t = zero). The validity of eqn. (13) was tested by plotting the reciprocal of the EPR signal height (which is proportional to $[^{t}\mathrm{BuOO}^{\bullet}]$) against the factor by which t is increased at each flow rate relative to the highest flow rate used (*e.g.*, at a flow rate of 30 ml min^{-1}, t will be 15-fold higher than its value at 2 ml min^{-1}). A straight-line plot was obtained [Fig. 5(a)], confirming the validity of the equation. Plots to test the model in which radical generation is

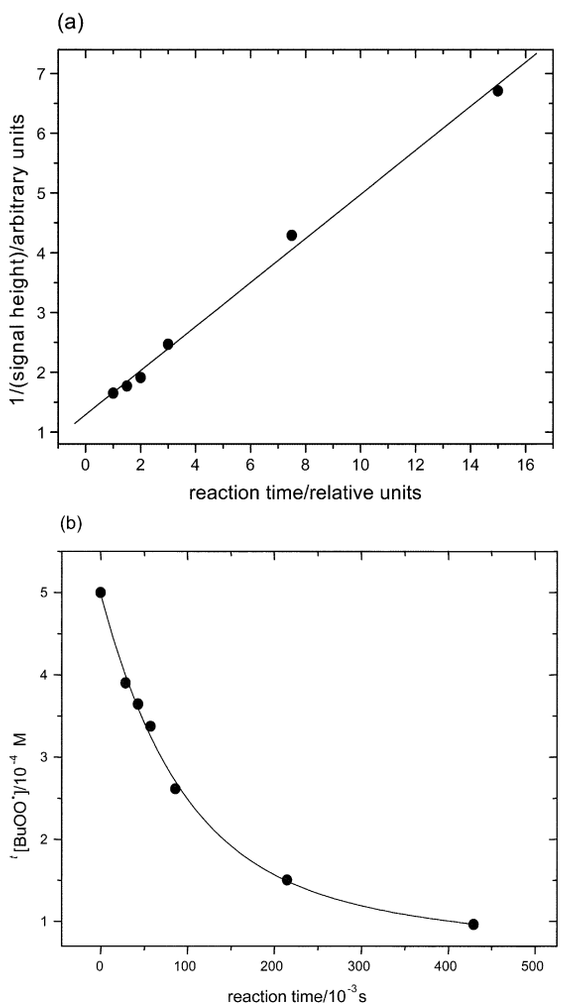

Fig. 5 Kinetics of ^{t}BuOO$^{\bullet}$ radical decay observed by continuous-flow EPR spectroscopy. (a) Second-order plot of ^{t}BuOO$^{\bullet}$ decay using arbitary units of signal intensity and relative units of reaction time; (b) variation of $[^{t}\mathrm{BuOO}^{\bullet}]$ with reaction time. See text for details.

still occurring at the point of EPR observation (see Czapski *et al.*[32]) were not satisfactory and therefore ruled out this kinetic description.

From the intercept of the *y*-axis of the plot shown in Fig. 5(a), a value of 775 (arbitrary units) is obtained for $[^tBuOO^\bullet]_o$. Since formation of the peroxyl radical occurs immediately upon reactant mixing, $[^tBuOO^\bullet]_o$ can be assumed to be equal to the concentration of Ce^{IV} at reaction time zero, $[Ce^{IV}]_o$ (0.5 mM). Using these numbers, absolute values of $1/([^tBuOO^\bullet]_t)$ were calculated for the data points reported in Fig. 5(a). Since the gradient obtained from a plot of $1/([^tBuOO^\bullet]_t)$ against the absolute reaction time is equal to $2k_{12}$, eqn. (13), which is reported to be 2×10^4 M^{-1} s^{-1},[29] the value for t at the maximum flow rate used (30 ml min^{-1}) is ~ 29 ms, from which the value achieved at each of the other flow rates used was calculated [Fig. 5(b)].

Spin-trapping studies

When Ce^{IV} (1 mM) was flowed against a solution containing excess ^{t}BuOOH (0.5 M) in the presence of 100 mM DMPO at a combined flow rate of 30 ml min^{-1} (t ~ 29 ms), a signal from a radical adduct was observed [simulated using a(N) = 1.38 mT, a(β-H) = 1.05 mT, a(γ-H) = 0.13 mT], which was partially obscured by the stronger $^tBuOO^\bullet$ signal (Fig. 6). Reducing the

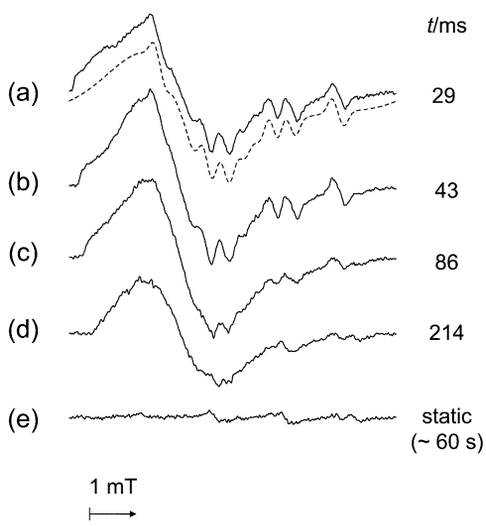

Fig. 6 EPR spectra observed following the mixing of 0.5 mM Ce^{IV} with 0.25 M ^{t}BuOOH in the presence of 50 mM DMPO (final, post-mixing concentrations). Spectra were recorded at the indicated reaction times by variation of the flow rate. The broken line under trace (a) is a computer simulation of the spectrum, consisting of the $^tBuOO^\bullet$ radical (96.5 % relative area), DMPOX [a(N) = 0.72 mT, a(β-H)(2) = 0.41 mT] (0.6 % relative area) and a nitroxide assigned to DMPO–$^\bullet$OO^tBu [a(N) ~1.38 mT, a(β-H) ~1.05 mT, a(γ-H) = 0.13 mT] (2.9 % area). See text for details.

flow rate (*i.e.*, increasing t) resulted in a decrease in the intensity of the signal from the nitroxide. When the flow was stopped, a very weak signal from a relatively stable radical adduct was detected [simulated using a(N) = 1.48 mT, a(β-H) = 1.59 mT], which was clearly distinct from that observed whilst flowing.

In order to investigate in more detail the radical adducts generated under *static* conditions, experiments were repeated at higher reagent concentrations in a quartz flat-cell positioned in a high-sensitivity cylindrical cavity. As shown in Fig. 7(a), the spectrum recorded within ~ 5 min of the mixing of 5 mM Ce^{IV}, 0.25 M ^{t}BuOOH and 0.8 M DMPO contained signals from at least three species. On the basis of the hfcc values obtained by computer simulation (not shown), these were identified as DMPO–$^\bullet$OMe [a(N) = 1.39 mT, a(β-H) = 1.09 mT, a(γ-H) = 0.13 mT], DMPO–$^\bullet$O^{t}Bu [a(N) = 1.48 mT, a(β-H) = 1.57 mT] and the DMPO oxidation product 5,5-dimethyl-1-pyrrolidone-2-oxyl (DMPOX, Fig. 1)[13] [a(N) = 0.72 mT, a(β-H)(2) = 0.41

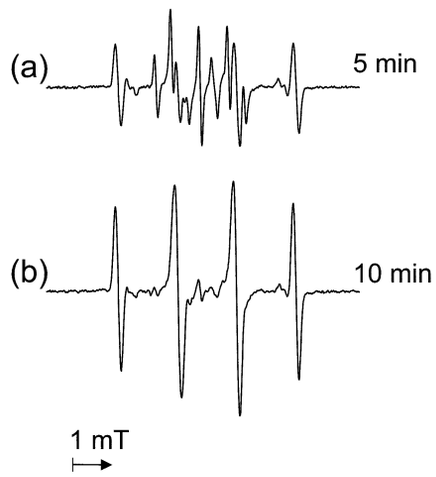

Fig. 7 Spectra obtained from a reaction system containing 5 mM Ce^{IV}, 0.25 M ^{t}BuOOH and 0.8 M DMPO. Spectra were recorded at the times indicated using a standard quartz flat-cell and a cylindrical resonator. Spectrum (a) consists of signals assigned to DMPO–$^\bullet$OMe [a(N) = 1.39 mT, a(β-H) = 1.09 mT, a(γ-H) = 0.13 mT] (18.2 % relative area), DMPOX [a(N) = 0.72 mT, a(β-H)(2) = 0.41 mT] (35.4 % relative area) and DMPO–$^\bullet$O^{t}Bu [a(N) = 1.48 mT, a(β-H) = 1.57 mT] (46.4 % relative area). Spectrum (b) is dominated by the signal from DMPO–$^\bullet$O^{t}Bu.

mT], in the percentage proportions 18.2, 46.4 and 35.4%. When Ce^{IV} and DMPO were mixed under static conditions in the absence of ^{t}BuOOH, a strong signal from DMPOX was observed (not shown), suggesting that the formation of this species involves the initial oxidation of DMPO to a radical cation by the metal ion, followed by hydrolysis and subsequent two-electron oxidation (Scheme 1). This is supported by the findings of a recent study by Clément *et al.*, involving the DMPO analogue 5-(diethoxyphosphoryl)-5-methyl-1-pyrroline *N*-oxide (DEPMPO). These workers observed, together with a strong signal from DEPMPOX, a weak signal from DEPMPO–$^\bullet$OH following the oxidation of DEPMPO by Ce^{IV}.[33] (It is, of course, possible that DMPOX may also be generated by a mechanism involving the peroxide, which will be addressed below.) When a second spectrum was recorded on the static sample (t ~ 10 min), DMPOX and DMPO–$^\bullet$OMe were seen to have decayed, whereas the signal from DMPO–$^\bullet$O^{t}Bu had doubled in intensity [Fig. 7(b)]. It is apparent, therefore, that the predominant signal present in Fig. 6(e) is from DMPO–$^\bullet$O^{t}Bu.

Although the computer simulation of the spectrum shown in Fig. 6(a), containing signals from the *unstable* adduct, DMPOX and the free $^tBuOO^\bullet$ radical, is a reasonable fit, satisfactory simulations could also be obtained by slightly varying the hfcc values of the unstable adduct from those reported in the figure legend. Due to the close similarity between these hfcc values and those of the DMPO–$^\bullet$OMe adduct,[19,34] it would be very difficult, solely on such a basis, to conclude that the unstable adduct is not DMPO–$^\bullet$OMe. However, we believe this species is not DMPO–$^\bullet$OMe for two principal reasons. Firstly, the nitroxide is very unstable, undergoing decay within ~ 0.2 s, yet the authentic DMPO–$^\bullet$OMe adduct is known to be stable (persisting for at least 5 min under the conditions reported in Fig. 7). This is consistent with the proposals of Dikalov and Mason, who showed that various peroxyl radical adducts of DMPO cannot be detected at room temperature under static conditions.[19] Secondly, the failure to detect a signal from the DMPO–$^\bullet$O^{t}Bu adduct under fast-flow conditions is inconsistent with the generation of DMPO–$^\bullet$OMe [Figs. 6(a) and (b)]. The methyl radical, and hence DMPO–$^\bullet$OMe, cannot be generated from ^{t}BuOOH other than *via* β-scission of the *tert*-butoxyl radical; see reaction (3) and also reactions (4) to (9) above.

$$(CH_3)_3CO^\bullet \longrightarrow (CH_3)_2CO + {}^\bullet CH_3 \qquad (3)$$

Given that the rate constant for the trapping of $^{\bullet}O^{t}Bu$ by DMPO is ~ 10^7 M^{-1} s^{-1} in aqueous solution,[35] and that the rate constant for the competing β-scission reaction (k_3) of the *tert*-butoxyl radical is 1.5×10^6 s^{-1},[35] it is difficult to see how we could have observed DMPO–$^{\bullet}$OMe without also seeing DMPO–$^{\bullet}O^{t}Bu$ in the presence of 50 mM spin trap [Figs. 6(a) and (b)]. Indeed, the DMPO–$^{\bullet}O^{t}Bu$ adduct is stable for at least 10 min and has a spectrum that is readily distinguished from that of DMPO–$^{\bullet}$OMe (Fig. 7). It is concluded, therefore, that the unstable nitroxide observed is DMPO–$^{\bullet}OO^{t}Bu$. The close similarity of the spectra from DMPO–$^{\bullet}$OMe and DMPO–$^{\bullet}OO^{t}Bu$ reflects the recently reported similarity between the spectra of peroxyl radical adducts of DEPMPO and DEPMPO–$^{\bullet}$OMe.[36,37]

In systems employing powerful one-electron oxidants, such as Ce^{IV}, it is always necessary to consider the possibility of radical adduct generation by 'inverted' spin-trapping, in which oxidation of the spin trap to a radical cation is followed by the addition of a nucleophile (as shown for the generation of DMPO–$^{\bullet}$OH in Scheme 1).[38,39] Thus, it could be argued that formation of the DMPO–$^{\bullet}OO^{t}Bu$ adduct observed here involves the nucleophilic addition of ^{t}BuOOH to the DMPO radical cation. When continuous-flow experiments were performed using DMPO in 10-fold excess over the peroxide (50 mM DMPO, 5 mM ^{t}BuOOH and 0.25 mM Ce^{IV}), to favour DMPO oxidation to its radical cation, a prominent signal from DMPOX was observed in addition to that from $^{t}BuOO^{\bullet}$ (not shown). However, only an extremely weak signal from DMPO–$^{\bullet}OO^{t}Bu$ was seen under these conditions, which is inconsistent with its generation *via* inverted spin-trapping. The low yield of DMPO–$^{\bullet}OO^{t}Bu$ observed under these conditions is believed to reflect the lower yield of $^{t}BuOO^{\bullet}$ radicals and the slow rate of their reaction with DMPO (*vide infra*). The omission of DMPO from the above experiment resulted in a moderate increase in the intensity of the signal from the free $^{t}BuOO^{\bullet}$ radical (from 2.1 to 2.9 arbitrary units). Assuming that the lower [$^{t}BuOO^{\bullet}$] seen in the presence of DMPO reflects only the competition between the spin trap and ^{t}BuOOH for reaction with Ce^{IV}, then the decrease in intensity of the $^{t}BuOO^{\bullet}$ signal in the presence of the spin trap is described by eqn. (14),[40,41]

$$I_o/I_{DMPO} = 1 + k_{DMPO}[DMPO]/k_{11}[\,^{t}BuOOH] \quad (14)$$

in which I_o is the intensity of the $^{t}BuOO^{\bullet}$ signal observed in the absence of DMPO, I_{DMPO} the intensity of the signal observed in the presence of the spin trap, k_{DMPO} the second-order rate constant for the reaction of Ce^{IV} with DMPO and k_{11} the rate constant for the oxidation of ^{t}BuOOH by Ce^{IV} [reaction (11)]. Using the value for k_{11} determined above by stopped-flow electronic absorption spectroscopy (1.3×10^4 M^{-1} s^{-1}), the upper limit for the rate constant for the reaction of Ce^{IV} with the spin trap was estimated to be 500 M^{-1} s^{-1}. It is concluded, therefore, that because ^{t}BuOOH is oxidised by Ce^{IV} much more readily than DMPO, the DMPO–$^{\bullet}OO^{t}Bu$ adduct is not generated by inverted spin-trapping under the conditions of excess ^{t}BuOOH employed in Fig. 6. This is supported by the findings of Eberson, who has shown that inverted spin-trapping occurs much more readily with the acylic nitrone α-phenyl-*N*-*tert*-butylnitrone (PBN) than with DMPO. This is believed to be because PBN is oxidised to a radical cation at a potential about 0.2 V lower than DMPO.[39] Even in the presence of the powerful one-electron oxidant $OsCl_6^-$, for which the standard reduction potential (Os^{V}/Os^{IV}) is very similar to that of the Ce^{IV}/Ce^{III} couple employed here, increasing the potential at which PBN is oxidised through 4-nitro substitution cuts down the incidence of inverted spin-trapping considerably.[38]

Although we have shown clearly that Ce^{IV} can oxidise DMPO to DMPOX, it is possible that the nitroxide may also be generated during the decomposition of the DMPO–$^{\bullet}OO^{t}Bu$ adduct. Indeed, other workers have reported the detection of DMPOX during the oxidation of both ^{t}BuOOH and cumene hydroperoxide.[13,17] The mechanisms of DMPOX formation proposed in these earlier studies are not applicable to the reaction conditions applied here. It is, therefore, considered likely that DMPO peroxyl radical-adducts can undergo decomposition by various mechanisms depending, for example, on the oxidant used to bring about the initial oxidation of the peroxide. In the reaction system employed here, it is possible that this involves the homolytic cleavage of the radical adduct, followed by oxidation of the resultant nitrone by Ce^{IV} (Scheme 1). It is certainly the case that DMPOX is not always detected in peroxyl radical generating systems employing DMPO as a spin trap, but this may reflect the absence of a sufficiently powerful oxidant for the final oxidation step. Clearly, further studies are required into the mechanism of peroxyl radical adduct decomposition.

Our findings and conclusions are in marked contrast with those of recent investigations by Honeywill and Mile.[42] These authors photolysed di-*tert*-butyl peroxide ($^{t}BuOO^{t}Bu$) in the presence of oxygen to generate tertiary alkylperoxyl radicals ($^{t}ROO^{\bullet}$) from 2-methylbutane. By maintaining the temperature below 155 K, a steady state concentration of the radicals was achieved, in equilibrium with the tetraoxide as given in reaction (15).

$$2\ ^{t}ROO^{\bullet} \rightleftharpoons\ ^{t}ROOOO^{t}R \quad (15)$$

This is because the activation energy for the decomposition of the tetraoxide back to two $^{t}ROO^{\bullet}$ radicals is lower than that for its decomposition to O_2 plus either two $^{t}RO^{\bullet}$ radicals or one $^{t}ROOtR$ molecule, which is the usual route of peroxyl radical bimolecular decay [see reaction (12), above, which is believed to proceed through a tetraoxide intermediate].[1,10,43,44] Upon the injection of a chilled solution of DMPO, Honeywill and Mile observed the rapid and complete removal of the signal from $^{t}ROO^{\bullet}$, which was not replaced by a signal from a nitroxide. However, when the temperature was raised to 200 K, a signal from the corresponding alkoxyl radical adduct (DMPO–$^{\bullet}O^{t}R$) was detected. They suggested that a diamagnetic (EPR-silent) product is generated upon $^{t}ROO^{\bullet}$ scavenging by DMPO, probably involving the addition of two $^{t}ROO^{\bullet}$ radicals to the spin trap and that, at higher temperature, this decomposes to DMPO–$^{\bullet}O^{t}R$.[42]

From our own findings and those of Dikalov and Mason,[19,20,37] it is likely that any peroxyl radical adduct generated under the conditions used by Honeywill and Mile would have been too unstable to reach an EPR-detectable concentration (not withstanding the lower temperature used by these authors). These workers suggested that the rate constant for the reaction of alkylperoxyl radicals with DMPO is (at least) 10^3 to 10^4 M^{-1} s^{-1}.[42] This was of obvious concern to us because it is inconsistent with the observation that DMPO resulted in only a small decrease in the intensity of the $^{t}BuOO^{\bullet}$ signal (g ~ 2.015) when present under fast-flow conditions. For example, in the spectrum recorded ~ 43 ms following the mixing of Ce^{IV} and ^{t}BuOOH in the presence of 50 mM DMPO (Fig. 6), the concentration of free $^{t}BuOO^{\bullet}$ radicals was estimated, from the signal height, to be 0.33 mM (see Fig. 5). When the experiment was carried out in the absence of DMPO, the concentration $^{t}BuOO^{\bullet}$ radicals observed at this time point was ~ 0.36 mM (not shown). Under the conditions of [^{t}BuOOH] > [DMPO] employed, and because the rate constant for the reaction of Ce^{IV} with ^{t}BuOOH is much greater than that for its reaction with DMPO (*vide supra*), it is reasonable to attribute the decrease in [$^{t}BuOO^{\bullet}$] brought about by the inclusion of DMPO to its trapping of the radical. In the absence of the spin trap, $^{t}BuOO^{\bullet}$ will decay primarily by the bimolecular process described above in reaction (12), $2k_{12} = 2 \times 10^4$ M^{-1} s^{-1}, as confirmed by the data shown in Fig. 5(a). However, in the presence of DMPO, a

Table 1 Second-order rate constants for the trapping of oxygen-centred radicals by DMPO

Radical	Rate constant/M^{-1} s^{-1}	Reference
$HOO^{\bullet}$	6.6×10^3	Finkelstein *et al.*[47]
$O_2^{\bullet -}$	10	Finkelstein *et al.*[47]
^{t}BuOO$^{\bullet}$	~30	This work
$HO^{\bullet}$	3.4×10^9	Finkelstein *et al.*[47]
^{t}BuO$^{\bullet}$	$\sim 7 \times 10^6$	Bors *et al.*[35]

proportion of the radical will also be lost through the spin-trapping reaction [reaction (2)].

$$2(CH_3)_3COO^{\bullet} \longrightarrow \text{products} \quad (12)$$

$$(CH_3)_3COO^{\bullet} + DMPO \longrightarrow DMPO\text{–}^{\bullet}OOC(CH_3)_3 \quad (2)$$

Since the concentration of DMPO is much greater than the concentration of ^{t}BuOO$^{\bullet}$ radicals, reaction (2) can be treated as a pseudo first-order reaction ($k'_2 = k_2$[DMPO]). By application of a standard, integrated rate law describing the parallel bimolecular decay of ^{t}BuOO$^{\bullet}$ [reaction (12)] and its scavenging by DMPO [reaction (2)], †[45,46] and assuming that the concentration of ^{t}BuOO$^{\bullet}$ at time zero is equal to the initial concentration of Ce^{IV} ions (*vide supra*), k_2 can be shown to be *ca.* 30 M^{-1} s^{-1}. Although much lower than the value proposed by Honeywill and Mile, this figure appears more reasonable when compared with the rate constants (k_{DMPO}) for the trapping of other oxygen-centred radicals (Table 1): replacement of the hydrogen atom in the hydroperoxyl radical ($HOO^{\bullet}$) with a *tert*-butyl group results in the lowering of k_{DMPO} by over two orders of magnitude, which is similar to the reduction in k_{DMPO} seen following the corresponding substitution in the hydroxyl radical ($HO^{\bullet}$, giving ^{t}BuO$^{\bullet}$). Indeed, it is considered highly unlikely that the rate constant for the trapping of tertiary peroxyl radicals suggested by Honeywill and Mile (at least 10^3 to 10^4 M^{-1} s^{-1})[42] is as great as that for the trapping of the more reactive $HOO^{\bullet}$ radical (6.6×10^3 M^{-1} s^{-1}).[47] Without further information, it would be difficult to provide an explanation for the very high value of k_{DMPO} obtained for tertiary alkylperoxyl radicals by Honeywill and Mile. We note, however, that these authors observed a considerable loss of resonator Q upon injecting into the sample tube once a steady state of ^{t}ROO$^{\bullet}$ radicals had been achieved (serious loss of signal occurred even with a blank, solvent injection). This, together with the reported 35 s reaction 'dead time', may account for the apparently high rate of ^{t}ROO$^{\bullet}$ loss.

Conclusions

1. The reaction between Ce^{IV} and ^{t}BuOOH in 0.4 M H_2SO_4 proceeds with a second-order rate constant of 1.3×10^4 M^{-1} s^{-1}. The observed reaction stoichiometry of 2:1 ([Ce^{IV}]:[^{t}BuOOH]) suggests that the ^{t}BuOO$^{\bullet}$ radicals generated upon oxidation of the peroxide by the first Ce^{IV} equivalent undergo oxidation by the second metal equivalent. Further studies are required to identify the end-products of this reaction. Under the conditions of excess peroxide used here, decay of the peroxyl radicals was by bimolecular self-reaction.

2. The reaction between the ^{t}BuOO$^{\bullet}$ radical and the spin trap DMPO results in the generation of a radical adduct (DMPO–$^{\bullet}$OO^{t}Bu), which decays within *ca.* 0.2 s. Due to poor spectral resolution, it was not possible to demonstrate a significant difference between the hfcc values for this adduct and those of the far more stable DMPO–$^{\bullet}$OMe adduct. The decomposition of DMPO–$^{\bullet}$OO^{t}Bu results in the release of the $^{\bullet}$O^{t}Bu radical, which may be trapped by excess DMPO or undergo β-scission to the methyl radical. The DMPO oxidation product DMPOX also appears to be generated during DMPO–$^{\bullet}$OO^{t}Bu breakdown, for which a possible reaction mechanism has been suggested (Scheme 1).

3. The second-order rate constant for the trapping of the ^{t}BuOO$^{\bullet}$ radical by DMPO was estimated to be *ca.* 30 M^{-1} s^{-1}. Though this figure is based on only limited data, it is clear that the value of (at least) 10^3–10^4 M^{-1} s^{-1} reported elsewhere is unrealistically high.[42]

4. Due (in part) to the low rate of reaction between Ce^{IV} and DMPO (< 500 M^{-1} s^{-1}), the possibility of DMPO–$^{\bullet}$OO^{t}Bu formation by inverted spin-trapping was ruled out under the reaction conditions reported here.

Acknowledgements

The authors are grateful to L. Folkes for assistance with the stopped-flow electronic absorption measurements and to P. Wardman, M. Naylor and W. Russell for helpful discussions. Financial support from Cancer Research UK is gratefully acknowledged. Thanks are also extended to a referee who suggested that DMPOX may be generated during the decomposition of DMPO–$^{\bullet}$OO^{t}Bu.

References

1 K. U. Ingold, *Acc. Chem. Res.*, 1969, **2**, 1.
2 M. J. Perkins, *Radical Chemistry*, Ellis Horwood, London, 1994.
3 C. von Sonntag and H.-P. Schuchmann, *Angew. Chem., Int. Ed. Engl.*, 1991, **30**, 1229.
4 B. Halliwell and J. M. C. Gutteridge, *Free Radicals in Biology and Medicine*, Oxford University Press, Oxford, 3rd edn., 1989.
5 M. J. Burkitt, *Arch. Biochem. Biophys.*, 2001, **394**, 117.
6 C. von Sonntag and H.-P. Schuchmann, in *Peroxyl Radicals*, ed. Z. B. Alfassi, John Wiley & Sons Ltd., London, 1997, p. 173.
7 W. Chamulitrat and R. P. Mason, *J. Biol. Chem.*, 1989, **264**, 20968.
8 W. T. Dixon and R. O. C. Norman, *Nature*, 1962, **196**, 891.
9 J. E. Bennett and R. Summers, *J. Chem. Soc., Faraday Trans. 2*, 1973, **69**, 1043.
10 J. R. Thomas, *J. Am. Chem. Soc.*, 1965, **87**, 3935.
11 B. Kalyanaraman, C. Mottley and R. P. Mason, *J. Biol. Chem.*, 1983, **258**, 3855.
12 G. R. Buettner, *Free Radical Biol. Med.*, 1987, **3**, 259.
13 G. M. Rosen and E. J. Rauckman, *Mol. Pharmacol.*, 1980, **17**, 233.
14 M. J. Davies, *Biochem. J.*, 1989, **257**, 603.
15 G. S. Timmins and M. J. Davies, *Carcinogenesis*, 1993, **14**, 1615.
16 C. H. Kennedy, D. F. Church, G. W. Winston and W. A. Pryor, *Free Radical Biol. Med.*, 1992, **12**, 381.
17 P. J. Thornalley, R. J. Trotta and A. Stern, *Biochim. Biophys. Acta*, 1983, **759**, 16.
18 C. Rota, D. P. Barr, M. V. Martin, F. P. Guengerich, A. Tomasi and R. P. Mason, *Biochem. J.*, 1997, **328**, 565.
19 S. I. Dikalov and R. P. Mason, *Free Radical Biol. Med.*, 1999, **27**, 864.
20 S. I. Dikalov and R. P. Mason, *Free Radical Biol. Med.*, 2001, **30**, 187.
21 J. A. Howard and J. C. Tait, *Can. J. Chem.*, 1978, **56**, 176.
22 E. G. Janzen, P. H. Krygsman, D. A. Lindsay and D. L. Haire, *J. Am. Chem. Soc.*, 1990, **112**, 8279.
23 J. Karlsson, M. Emgård, P. Brundin and M. J. Burkitt, *J. Neurochem.*, 2000, **75**, 141.
24 S. P. Wolff, *Methods Enzymol.*, 1994, **233**, 182.
25 C. Gay and J. M. Gebicki, *Anal. Biochem.*, 2000, **284**, 217.
26 R. J. Faber and G. K. Fraenkel, *J. Chem. Phys.*, 1967, **47**, 2462.
27 D. R. Duling, *J. Magn. Reson., Ser. B*, 1994, **104**, 105.
28 J. R. Thomas and K. U. Ingold, *Advances in Chemistry Series*, 1968, No. 75, American Chemical Society, p. 258.
29 J. E. Bennett, *J. Chem. Soc., Faraday Trans.*, 1990, **86**, 3247.

† The integrated rate equation for the combined decay of ^{t}BuOO$^{\bullet}$ by reactions (12) and (2) is,

$$\ln[c/(1 + 2rc)] = -k'_2 t + \ln[c_o/(1 + 2rc_o]$$

where c is the concentration of ^{t}BuOO$^{\bullet}$ at time t, c_o the concentration of the radical at time zero and r is k_{12}/k'_2 (see refs. 45 and 46 for details).

30 F. A. Cotton and G. Wilkinson, *Advanced Inorganic Chemistry*, Wiley-Interscience, 5th edn., New York, 1988.
31 B. C. Gilbert, J. K. Stell and M. Jeff, *J. Chem. Soc., Perkin Trans. 2*, 1988, 1867.
32 G. Czapski, *J. Phys. Chem.*, 1971, **75**, 2957.
33 J.-L. Clément, B. C. Gilbert, A. Rockenbauer and P. Tordo, *J. Chem. Soc., Perkin Trans. 2*, 2001, 1463.
34 M. J. Burkitt, S. Y. Tsang, S. C. Tam and I. Bremner, *Arch. Biochem. Biophys.*, 1995, **323**, 63.
35 W. Bors, C. Michel and K. Stettmaier, *J. Chem. Soc., Perkin Trans. 2*, 1992, 1513.
36 J.-L. Clément, B. C. Gilbert, A. Rockenbauer, P. Tordo and A. C. Whitwood, *Free Radical Res.*, 2002, **36**, 883.
37 S. Dikalov and R. P. Mason, *Poster presented at the 7th International Symposium on Spin Trapping*, July 7–12, Chapel Hill, North Carolina, USA, 2002.
38 L. Eberson and M. Nilsson, *Acta Chem. Scand.*, 1993, **47**, 1129.
39 L. Eberson, *J. Chem. Soc., Perkin Trans. 2*, 1994, 171.
40 K.-D. Asmus, *Methods Enzymol.*, 1984, **105**, 167.
41 S. R. Logan, *Fundamentals of Chemical Kinetics*, Longman, Harlow, 1996.
42 J. D. Honeywill and B. Mile, *J. Chem. Soc., Perkin Trans. 2*, 2002, 569.
43 P. D. Bartlett and G. Guaraldi, *J. Am. Chem. Soc.*, 1967, **89**, 4799.
44 J. E. Bennett, D. M. Brown and B. Mile, *J. Chem. Soc., Faraday Trans.*, 1970, **66**, 397.
45 K. A. Connors, *Chemical Kinetics. The Study of Reaction Rates in Solution*, VCH, New York, 1990, p. 65.
46 C. Capellos, and B. H. J. Bielski, in *Kinetic Systems. Mathematical Description of Chemical Kinetics in Solution*, John Wiley & Sons, New York, 1972, p. 89.
47 E. Finkelstein, G. M. Rosen and E. J. Rauckman, *J. Am. Chem. Soc.*, 1980, **102**, 4994.